19th IMEKO TC10 Conference
"MACRO meets NANO in Measurement for Diagnostics, Optimization and Control"
Delft, The Netherlands , September 21–22, 2023

Anomaly Score for Multiple Operating Modes of Rotating Machines by Using Conditional Variational Auto-Encoder

Yukio Hiranaka[1,2], Koichi Tsujino[1], Hidenori Katsumura[3], Masashi Nakagawa[3]

[1] *AiSpirits Inc., Tokyo, Japan, yukio.hiranaka.at.aispirits.com*
[2] *Hiranaka Technology Research, Susono, Japan*
[3] *Device & System Platform Development Center Co., Ltd., Kawasaki, Japan*

***Abstract* – Human Experts may diagnose the state of a rotating machine by listening to its vibration sounds. Variational Auto-encoder (VAE) is an alternative method to realize the diagnosis by AI learning. Previous studies have shown that when the normal state can be assumed to be a single Gaussian distribution, anomaly scores can be calculated as deviations from the center of the distribution in the VAE latent space. However, when the normal state consists of different modes corresponding to operating conditions, the calculation may not be a simple task. As a way to solve this problem, the use of Conditional Variational Auto-encoder (CVAE) which performs VAE learning including operating conditions, seems promising. In this study, we show verification results that the anomaly score based on the normalized Euclidian distance in the CVAE latent space can detect anomalous conditions using synthesized data and real acceleration measurement data with rotation speed changes.**

Keywords – Conditional Variational Auto-encoder, Condition Based Maintenance, Bearing Anomaly Detection, Industry Innovation and Infrastructure.

I. INTRODUCTION

Anomaly detection methods are important for realizing condition based maintenance (CBM) of factory machines [1]. There are various types of anomaly, and it is necessary to determine the threshold for anomaly detection depending on the target and its states. Human experts can make judgments based on their experiences in various situations. Currently, one of the leading ways to realize this with AI is the VAE method, which calculates anomaly scores after learning the normal conditions [2,3,4].

In practice, as the normal state generally changes depending on the operating conditions (rotating speed, operating load, etc.), it is difficult to discriminate anomalies in consideration of the variation of all operating conditions [5]. Then, Conditional Variational Auto-encoder [6] (abbreviated as CVAE), which performs learning including operating conditions, is emerged as a promising method that can handle such cases [5,7,8].

In this study, we applied CVAE and examined the resulting distribution in its latent space for synthetic data and measured data. Also, the effectiveness of normalized Euclidean distance in the CVAE latent space as the anomaly score is verified. The paper consists of the description of the anomaly score calculation in section II, synthetic model data and results in section III, real measurement data and results in section IV, and conclusions.

II. VAE AND CONDITIONAL VAE

We briefly describe how to calculate anomaly scores using VAE [2]. The processing flow of the VAE is shown in Fig. 1. The VAE encoder generates latent variables with the specified number of dimensions D by learning a set of multidimensional training variable x_{km} (k and m represent the specific sample and the specific variable of the sample, respectively).

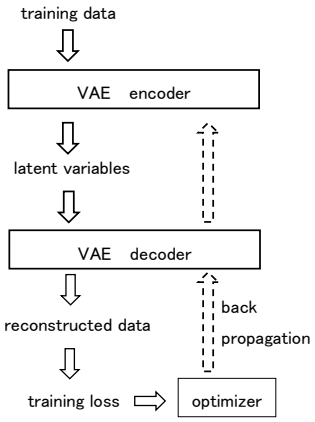

Fig. 1. Processing flow of the Variational Auto-encoder (VAE).

The latent variable z_{kd} (k and d represent the specific sample and the specific latent variable) that corresponds to each training sample is determined along the obtained latent space axes. The VAE decoder outputs the reconstructed variable x'_{km} corresponding to the original training variable x_{km}, and the backpropagation of the neural network is used to minimize the squared error between x_{km} and x'_{km} while constraining the distribution shape in the latent space to be Gaussian [9]. In the VAE processing, a virtual standard deviation v_{kd} of the latent variable z_{kd} is estimated. The estimation is converged so

that the average optimization can be realized with the perturbed values calculated by

$$z_{kd} + v_{kd}\varepsilon, \quad \varepsilon \in \mathrm{N}(0,1) \tag{1}$$

where N(0,1) represents the standard normal distribution.

Optimization is performed by minimizing the loss function (2), which corresponds to minimizing the reconstruction error in the first term and minimizing the KL divergence in the second term. This brings the distribution of decoder inputs (1) closer to the standard normal distribution.

$$loss = \frac{1}{s}\sum_{k=1}^{s}\left\{\sum_{m=1}^{M}|x'_{km} - x_{km}|^2 + \frac{1}{2}\sum_{d=1}^{D}(z_{kd}{}^2 + v_{kd}{}^2 - \ln v_{kd}{}^2 - 1)\right\}, \tag{2}$$

where S is the number of training samples and M is the number of sample variables.

Anomaly score V_D can be calculated as the normalized Euclidean distance from the center of the distribution [10],

$$V_D = \sqrt{\frac{1}{D_{cmps}}\sum_{d=1}^{D}\left(\frac{z_d - \overline{z_d}}{\sigma_d}\right)^2}, \tag{3}$$

$$D_{cmps} = \frac{1}{D}\sum_{i=1}^{D}\sum_{j=1}^{D} R^2(f_i, f_j), \tag{4}$$

$$R(f_i, f_j) = \frac{1}{M}\sum_{m=1}^{M} f_i(m)\, f_j(m), \tag{5}$$

where $\overline{z_d}$ is the mean value of z_d, σ_d is the standard deviation along the latent space axis d, D_{cmps} is the dimensionality compensation factor, $R(f_i, f_j)$ is the correlation coefficient between basis functions, and $f_i(m)$ is the m-th sample variable consisting the i-th basis function corresponding to the i-th latent axis [2].

When the input distribution is close to a single Gaussian distribution, the latent space distribution is also close to a Gaussian distribution, and the degree of anomaly can be evaluated by the distance from the center of the latent space distribution. However, when the input distribution is divided into multiple clusters or a belt-like transition (Fig. 2(a)) due to changes in operating conditions, the distance from the center of the entire distribution does not accurately represent the degree of anomaly. Ideally, we should evaluate the deviation from the ridge line of the normal condition as shown in Fig. 2(b). However, it is generally difficult to determine an applicable evaluation formula which properly expresses the distribution. Therefore, it is practical to divide the distribution into clusters of appropriate size and express the degree of anomaly by the distance from the center of each cluster as shown in Fig. 2(c).

To create a separate VAE for each operating condition is a way to do the division, but it not only complicates the training process, but also poses the challenge to classify operating conditions properly. On the other hand, with CVAE, we can train in a unified manner with one VAE, including the conditions. By providing one hot encoded conditions to CVAE, it is possible to move clusters to the center of the latent space [5]. Actually, with the effect of the VAE loss function (2), the distribution for each cluster gathers in one place as shown in Fig. 2(d), and the anomaly score is calculated based on the distance from the center regardless of the cluster to which the input sample belongs.

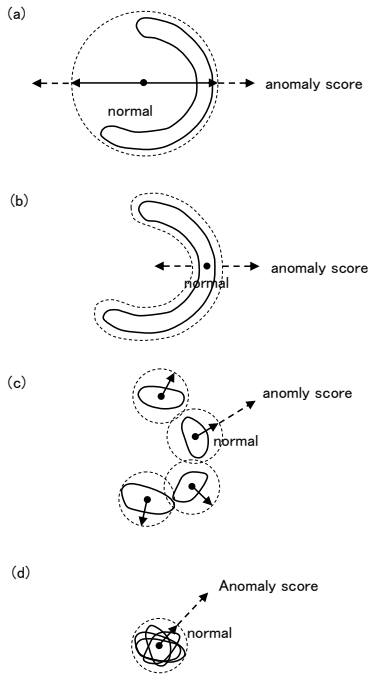

Fig. 2. Illustration of latent space distributions. (a) Points surrounded by normal state distributions become normal in VAE, (b) ideal anomaly judgment, (c) anomaly judgment for each cluster, (d) cluster movement by CVAE can unify the normal clusters.

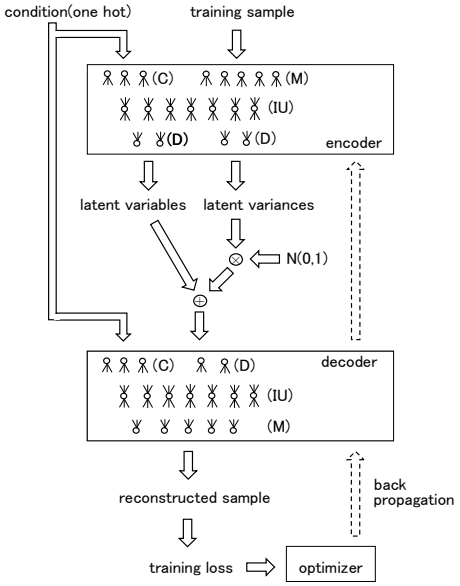

Fig. 3. Processing flow of the Conditional VAE (CVAE).

In CVAE processing, it is necessary to input operating conditions (rotational speed, load, etc.) as one hot encoded variables to the encoder and decoder together with other training sample variables or latent variables (Fig. 3). However, only the input variable x_{km} is compared with the reconstructed variable x'_{km} for the reconstruction error term (2) in the optimization.

III. MODEL SIMULATION

Firstly, we confirmed the effectiveness of CVAE under an ideal condition using synthetic data. As shown in Fig. 4, two dimensional random samples distributed in a semicircle was created with equations (6)-(9). It simulates, for example, a case in which x_0 and x_1 correspond to rotational speed and magnitude of vibration, respectively. The distribution expresses a phenomenon which shows intensified vibration at intermediate rotation speeds, as an example.

$$x_0 = 1 + \cos\frac{\pi i}{N} + 0.1\varepsilon_0, \quad (6)$$

$$x_1 = \sin\frac{\pi i}{N} + 0.1\varepsilon_1, \quad (7)$$

$$c = \left\lfloor 18\frac{i}{N} \right\rfloor, \quad (8)$$

$$\varepsilon_0, \varepsilon_1 \in \mathrm{N}(0,1), \quad (9)$$

where sample number $i = 0$ to N-1 ($N = 540$), condition value c=0 to 17 (number of conditions nc=18).

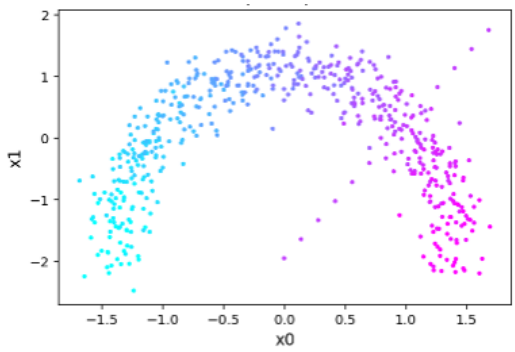

Fig. 4. Two dimensional distribution of synthetic samples. Color represents condition c (nc=18).

Fig. 5 shows that each condition has 30 samples, which is represented as the number of members nm=30 (set to be matched with section IV). A total of 13 points equally separeted on a slant line in Fig. 4, are test samples for confirming anomaly detection, whose condition values are the same to the crossing points in the distribution.

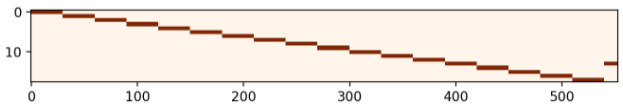

Fig. 5. Sequential change of condition values (vertical axis) in Fig.4.

The latent space distribution of the VAE has a shape similar to that in Fig. 4, and the test data points do not show a remarkable change in the anomaly score calculated as the distance from the distribution center (Fig. 6).

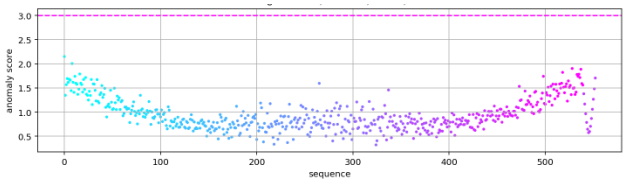

Fig. 6. VAE anomaly score for the case of Fig.4.

Fig. 7 shows the latent space distribution obtained by CVAE. Table.1 show the hyperparameter used, the input dimension M is 2, and the number of training points is 540. As the result of cluster-wise shifting illustrated in Fig. 2(d), the variance on both the horizontal and vertical axes become smaller. The test sample points appear as a slant line going out of the normal state distribution. At least seven outer sample points (five in the upper left and two in the lower right) can be easily detected as anomalies.

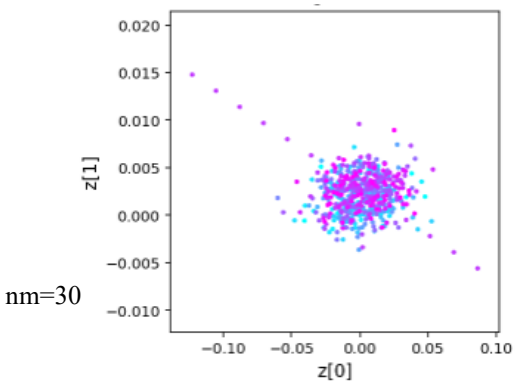

Fig. 7. Two dimensional CVAE latent space map for the case of Fig.4. Variables z[0] and z[1] correspond to the latent space axes.

Table 1. Hyperparameters for the VAE and the CVAE experimnts.

conditions (C)	18
layers	3
intermediate nodes (IU)	16
latent variables (D)	2
activation	linear
epochs	1,000
batch size	1
optimizer	Adam

Fig. 8. shows the anomaly score obtained from the latent variables in Fig.7 by formula (3). Anomaly scores of the six test samples at the trailing end are larger than 3σ (red horizontal line) of the training normal state distribution.

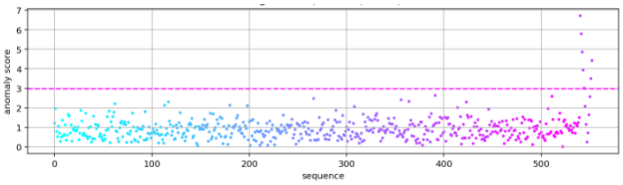

Fig. 8. CVAE anomaly score calculated from Fig.7.

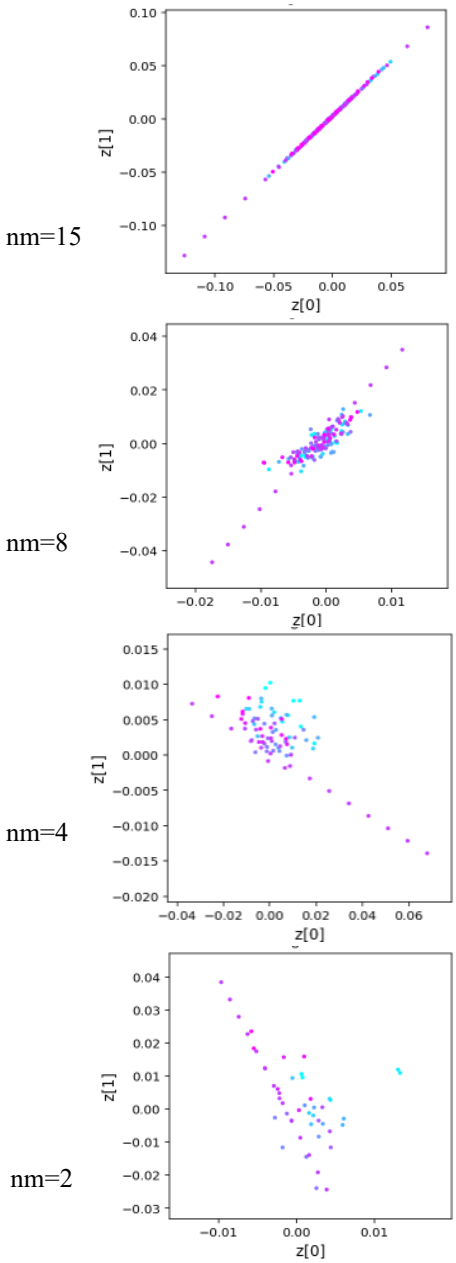

Fig. 9. CVAE latent space map for different number of members (nm) 15/8/4/2.

Fig.9 shows CVAE latent space distributions when the number of cluster members nm (=N/nc) for each condition is reduced to 15, 8, 4, and 2 to investigate the effect of training data size. If there are 4 or more sampes in each cluster, outer test samples can diverge greatly from the concentrated training distributions, similar to the distribution in Fig.7, though with some shape difference.

Fig.10 shows CVAE latent space distributions when the number of conditions nc is reduced to 10, 5, 3, 2 (settings are consistent with section IV measurement data). The total number of training samples is set to 540 so that the difference among distributions can be evenly observed. It can be seen that when nc increases, individuality of each cluster shape disappears and the anomaly score will be effective.

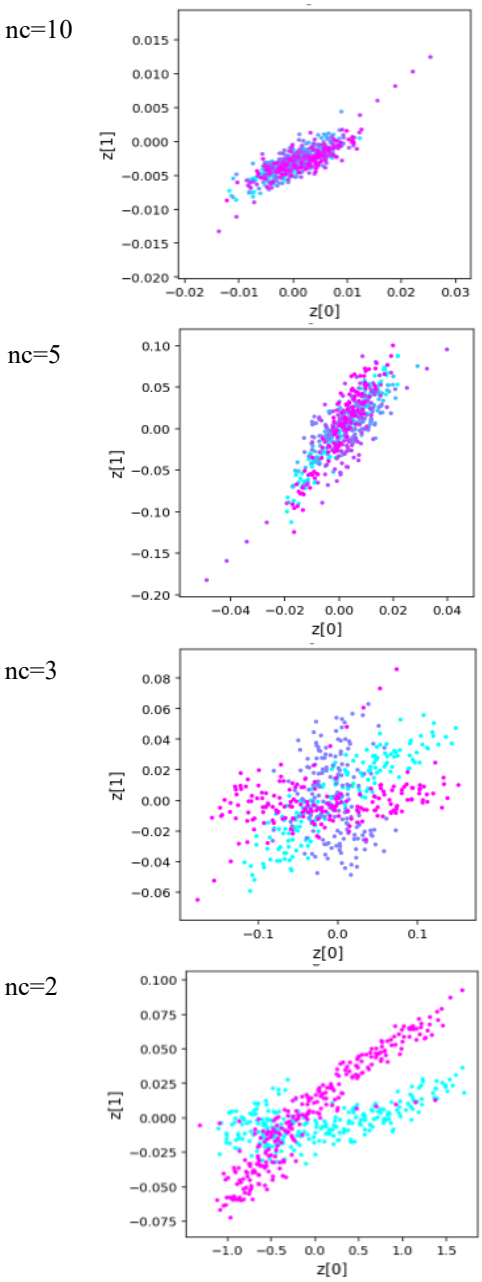

Fig. 10. CVAE latent space map for different number of conditions (nc) 10,5,3,2.

IV. REAL MESUREMENT

The CVAE method described in the former sections was applied to real measurement data to check its validity. The data was collected on an induction motor (15 kW) which drives a water pump installed in an air conditioning facility. The rotation speed of the motor is dynamically changed depending on the air conditioning load as a variable-frequency drive. Thus, we can obtain data at multiple rotation speeds.

An acceleration sensor was attached to the driving side bearing of the motor and used to collect 2048 time signals sampled at around 26kHz (count as one sample) once an hour. Then, each sample was converted to an amplitude spectrum (128 frequency points at around 100Hz intervals), and provided as parallel inputs to the CVAE encoder. A magnetic sensor was attached to the motor and used to collect alternating magnetic flux of the motor. Each sample of magnetic signals (once an hour) was also converted to an amplitude spectrum (128 frquency points at around 0.2Hz intervals). Actual rotation speeds quantized into 18 steps and converted to one hot encoded condition variables which were provided as the condition input (Fig. 11).

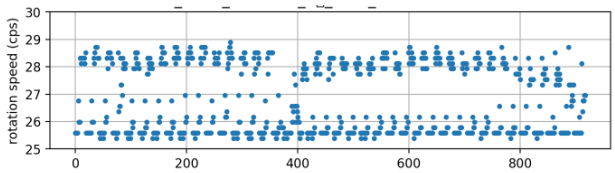

Fig. 11. Rotation speed quantized into 18 steps.

Hyperparameters for the CVAE are the same as Table.1 and the input dimension M is 128. The training samples are 540 points from the beginning of Fig. 11. The duration of the training samples is long compared to the total length because some rotation speeds do not appear or only appear a few times when we set the training duration shorter. If some condition-input samples were not included in the training data, the CVAE's latent variables would be indefinite. So, we have to include some number of all condition-input samples in the training data.

The sample at time sequence 565 corresponds to a rotation stop state, which we utilize to examine the quality of our anomaly score as it is a necessary condition for the sample to have a large deviation from the training samples.

Fig. 12 shows the resulting VAE latent space map, in which each cluster is distributed continuously in a V shape. The CVAE result (Fig. 13) shows concentration of clusters near the origin of the latent space. Although the shapes of constituent clusters slightly differ depending on rotation speeds, the distributions can be recognized as one cluster, roughy. The isolated point (light blue in the lower right) in Fig.12 corresponds to the rotation stop state. Regardless of the rotation speed classified for the state by the speed calculation program, it will be greatly deviated from the distribution, and the anomaly score (Fig. 14) for the state is also remarkable (the outlier at 565 on the horizontal axis).

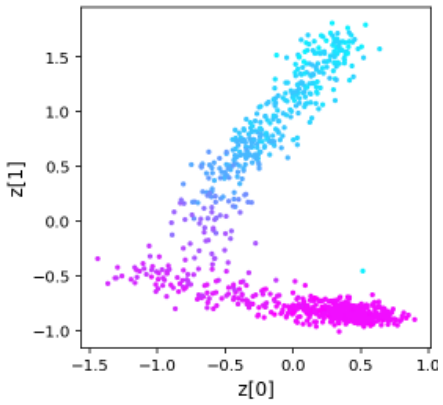

Fig. 12. VAE latent space map (nc=18, color-coded by rotation speed).

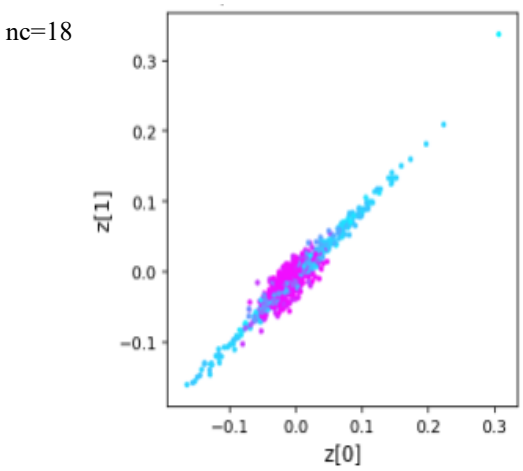

Fig. 13. CVAE latent space map corresponding to Fig.12.

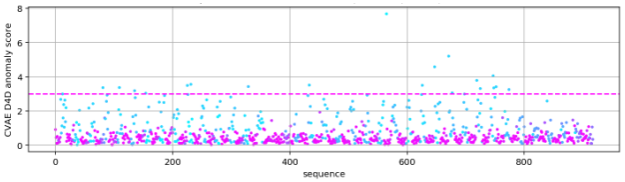

Fig. 14. Calculated anomaly score (540 training samples).

Fig.15 shows the CVAE latent space map when nc is reduced to 10, 5, 3, and 2. The reduction is performed by reducing magnetic frequency points changing the FFT size by half, repeatedly. And the resulting actual number of rotation speeds were 10, 5, 3 and 2. It can be seen that when the nc increases, individuality of each cluster shape disappears as in Fig.10. Basically, the larger the nc is, the farther the stopping point is clearly distinguishable from the training distribution.

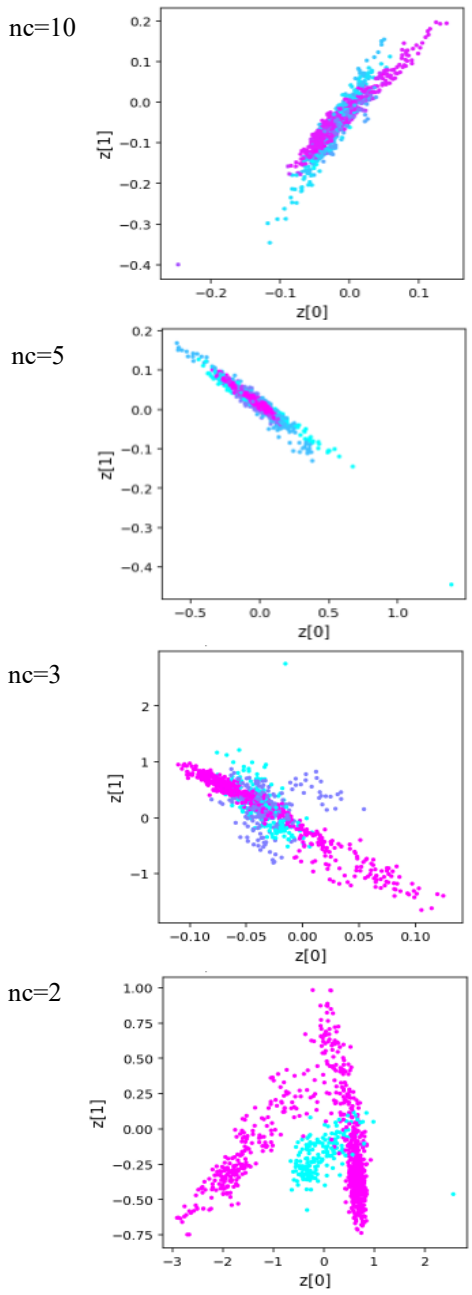

Fig. 15. CVAE latent space map for different number of conditions (nc) 10,5,3,2.

V. CONCLUSIONS AND FUTURE WORKS

It is shown that CVAE method is valid for a model simulation and a real measurement analysis. The distribution of CVAE latent space is concentrated into one smaller distribution regardless of operating condition, and the anomaly score calculated as the normalized Euclid distance from the center of the normal distribution is effective for anomaly detection. If the number of samples per cluster is sufficient, the larger the number of clusters, the higher the anomaly score converges.

Although we avoided the loss of training conditions by elongating training duration in section IV, there may be a possibility to interpolate non-existent condition-input by mixing two neiboring rotational spped conditions.

Some latent space maps show oblique elongated ellipse shape. As the normalized Euclid distance is not a suitable anomaly measure for such distributions, we need to calculate a kind of Mahalanobis' distance for smaller number of training samples and also with de-biasing functionality.

VI. ACKNOWLEDGMENT

This work was supported by the Cabinet Office (CAO), Cross-ministerial Strategic Innovation Promotion Program (SIP), "Intelligent Processing Infrastructure of Cyber and Physical Systems" (funding agency: NEDO).

REFERENCES

[1] **Randall, R.B.**, Vibration-based Condition Monitoring: Industrial, Aerospace and Automotive Applications, Wiley, 2ndEd, 2021.

[2] **Hiranaka, Y., Tsujino, K.**, VAE Deviation for Detecting Bearing Anomalies, 17th IMEKO TC 10 and EUROLAB Virtual Conference, October 20-22, 2020.

[3] **Zhang, S., Fei, Y., Wang, B., Habetler, T.G.,** Semi-Supervised Learning of Bearing Anomaly Detection via Deep Variational Autoencoders, 2019, arXiv:1912.01096v2.

[4] https://keras.io/examples/variational_autoencoder/

[5] **Lei, W.**, et al, Multiworking Conditions Anomaly Detection of Mechanical System Based on Conditional Variational Auto-Encoder, Hindawi Shock and Vibration Volume 2023, Article ID 2332669, https://doi.org/10.1155/2023/2332669, 2023.

[6] **Kingma, D.P., Rezende, D.J., Mohamed, S., Welling, M.**, Semi-supervised learning with deep generative models, Advances in Neural Information Processing Systems. 2014.

[7] **Zhao, X.**, et al., Normalized Conditional Variational Auto-Encoder with adaptive Focal loss for imbalanced fault diagnosis of Bearing-Rotor, Mechanical Systems and Signal Processing, DOI: 10.1016/j.ymssp.2022.108826, 2022.

[8] **Pol, A.A.**, et al., Anomaly Detection With Conditional Variational Autoencoders, 18th IEEE International Conference On Machine Learning And Applications (ICMLA), 2019.

[9] **Kingma, D.P., Welling, M.**, Auto-Encoding Variational Bayes, Proc. International Conference on Learning Representations, arXiv:1312.6114, 2014.

[10] **Kind, A., Stoecklin, M.P., Dimitropoulos, X.**, Histgram-Based Traffic Anomaly Detection, IEEE trans. Network Service Management, vol.6, no.2, pp.110-121 2009.